NOTES AND CORRESPONDENCE

A 6-Yr Climatology of Vertical Mean and Shear Components of Kinetic Energy for the Australian–South Pacific Jet Stream

MATTHEW D. EASTIN* AND DAYTON G. VINCENT

Department of Earth and Atmospheric Sciences, Purdue University, West Lafayette, Indiana

11 December 1996 and 4 June 1997

ABSTRACT

The climatology of the kinetic energy associated with the subtropical jet over the Australian–South Pacific region is investigated for a 6-yr period, January 1985–December 1990, using monthly mean data. The total kinetic energy (TKE) is partitioned into vertically averaged mean kinetic energy (KM) and level-by-level departure from the mean, or so-called shear kinetic energy (KS). A comparison of the two components during the annual cycle reveals that KM within the region of the subtropical jet is usually greater than KS. An out-of-phase relationship between the annual cycle of TKE and the annual cycle of the percentage of TKE represented by KS is found. A higher percentage of KS occurs in the summer season, when the jet is weakest. During late summer, KS dominates in the entrance region of the jet over Australia and the western Pacific. This appears to coincide with the annual strengthening of the jet. During winter, when the jet reaches its maximum intensity, KM dominates. It also dominates throughout the year in the exit region of the jet.

In addition, a comparison of TKE during an El Niño–Southern Oscillation cycle is made. Results indicate an increase of kinetic energy during El Niño over the central Pacific coupled with a decrease over Australia, indicating eastward movement of the jet. Subsequently, during La Niña, an opposite pattern is observed as the jet moves westward. The results of this climatological study, which appear to be in good agreement with the previous seasonal studies of the subtropical jet, could be beneficial to seasonal or year-to-year forecasting.

1. Introduction

The subtropical westerly jet stream over the Australian–South Pacific region and its accompanying jet streaks have received considerable attention in the last two decades (Huang and Vincent 1983, 1988; Paegle et al. 1983; Vincent 1985; Trenberth 1986, 1987; Nogues-Paegle and Zhen 1987; Nogues-Paegle and Mo 1988; Robertson et al. 1989; Hurrell and Vincent 1990, 1991; Smith and Bromwich 1994; Ko and Vincent 1995, 1996; Vincent et al. 1997). Figure 1 shows the 200-hPa zonal wind component for each of the four midseason months, based on 6-yr averages from 1985 to 1990. The subtropical jet varies considerably with season, both in speed and location. First, the jet has a large longitudinal extent in all seasons, except summer. Second, there is a double maximum in the jet core in all seasons except summer, one over western Australia and the other over the western Pacific. Third, in summer, there is a relatively weak maximum over the western Pacific, but no maximum over Australia.

In a recent study by Ko and Vincent (1995), the kinetic energy content of the subtropical jet over the South Pacific during the 1984–85 summer season was partitioned into its vertical mean and shear components (e.g., as in Wiin Nielsen 1962). The entrance and core regions of the jet were found to be dominated by shear kinetic energy, while the exit region appeared to have a higher percentage of mean kinetic energy. They also found a 1–2-week periodicity in the formation and propagation of the South Pacific jet streaks. In a subsequent paper, Ko and Vincent (1996) expanded their investigation to four 6-month summer periods from 1985 to 1989. Results of the latter study confirmed those from the 1984–85 summer season. In addition, they found that the mean position of the jet in 1986–87 (an El Niño year) was considerably farther east than it was in other years. Ko and Vincent did not address, however, the wintertime jet over the Australian–South Pacific region. The central theme of the present study, therefore, is to examine the annual variability, as well as the interannual variability of the kinetic energy content associated with the subtropical jet over the Australian–South Pacific region. Additionally, the total kinetic energy is partitioned into its vertical mean and shear components. Results will also be stratified as a function of latitude and longitude.

* Current affiliation: Department of Atmospheric Science, Colorado State University, Fort Collins, Colorado.

Corresponding author address: Dr. Dayton G. Vincent, Department of Earth and Atmospheric Sciences, Purdue University, 1397 Civil Engineering Building, West Lafayette, IN 47907-1397.
E-mail: dvincent@meteor.eas.purdue.edu

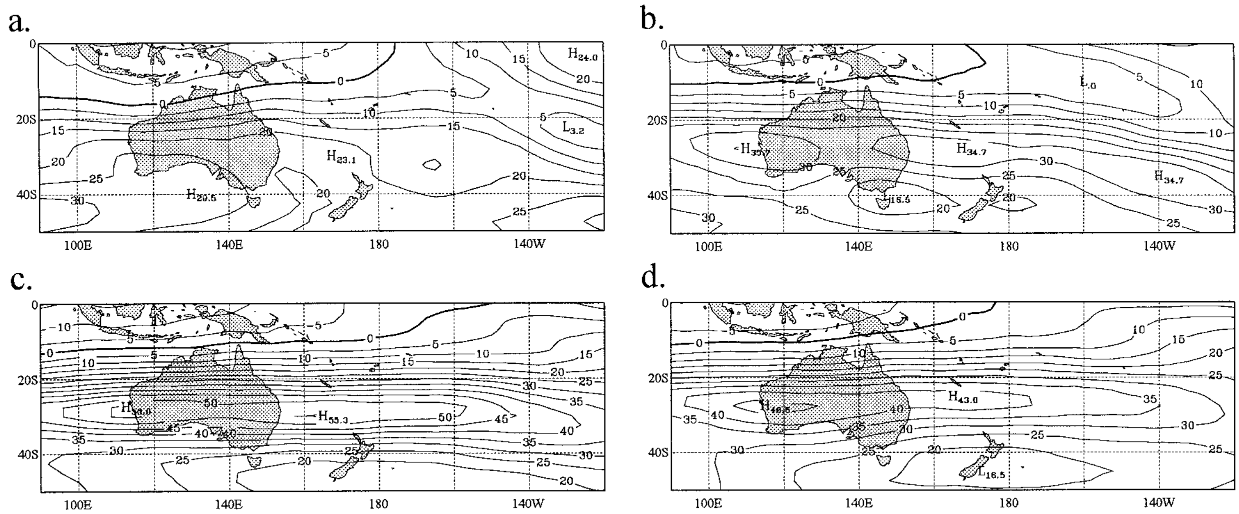

FIG. 1. Average zonal wind at 200 hPa in m s^{-1} for (a) January, (b) April, (c) July, and (d) October.

2. Data and kinetic energy equations

The data used in this study were European Centre for Medium-Range Weather Forecasts (ECMWF) global analyses taken from the World Climate Research Program and Tropical Ocean Global Atmosphere Archive II dataset. Trenberth (1992) provides an excellent evaluation and discussion of this dataset, which consists of uninitialized gridpoint values, available twice daily, for the horizontal winds, vertical p velocity, geopotential height, temperature, and relative humidity, with $2.5° \times 2.5°$ grid spacing at 14 mandatory levels. In this study only the horizontal wind data at the lowest 10 levels were processed (1000, 850, 700, 500, 400, 300, 250, 200, 150, 100 hPa) and these data were averaged between 0000 and 1200 UTC to compute daily values of kinetic energy and its components. The temporal domain covers the period from January 1985 to December 1990. A moderate El Niño (1986–87) and a moderate La Niña (1988–89) are contained within this period; thus, it is assumed that a reasonable representation of the longer-term climatology of the region is achieved. For further verification of this point, the reader is referred to the two atlases by Vincent and Schrage (1994, 1995) where the large-scale features of this region are discussed using the same climatology.

The area-averaged kinetic energy of a region, vertically integrated over the atmospheric mass, can be represented by

$$K = \frac{1}{gA}\iiint \frac{1}{2}(\mathbf{V}\cdot\mathbf{V})\,dx\,dy\,dp = \int_s\int_p k, \quad (1)$$

where

$\mathbf{V}$ = the horizontal wind vector,

A = the area of the region s,

$$\int_s\int_p = \frac{1}{gA}\iiint dx\,dy\,dp, \quad \text{and}$$

k = the horizontal kinetic energy per unit mass

$$= \frac{1}{2}(\mathbf{V}\cdot\mathbf{V}).$$

The kinetic energy in (1) can be partitioned into its vertical mean flow and its vertical shear flow, according to the method proposed by Wiin Nielson (1962). In this method, the vertically integrated mean of a variable is represented by

$$(\,)m = \frac{1}{\Delta p}\int_{p_t}^{p_o} (\,)\,dp, \quad (2)$$

where p_o and p_t are 1000 hPa and 100 hPa, respectively, and $\Delta P = p_o - p_t$. The integration is done using the trapezoidal method. The horizontal wind components are partitioned into their vertical mean and vertical shear (departure from the vertical mean at each level) components as follows:

$$u = u_m + u' \quad \text{and} \quad (3)$$

$$v = v_m + v'. \quad (4)$$

Using the above equations, the horizontal kinetic energy and its components per unit mass can be rewritten as

$$k = \frac{1}{2}(\mathbf{V}_m\cdot\mathbf{V}_m) + \frac{1}{2}(\mathbf{V}'\cdot\mathbf{V}') + \mathbf{V}_m\cdot\mathbf{V}', \quad (5)$$

where

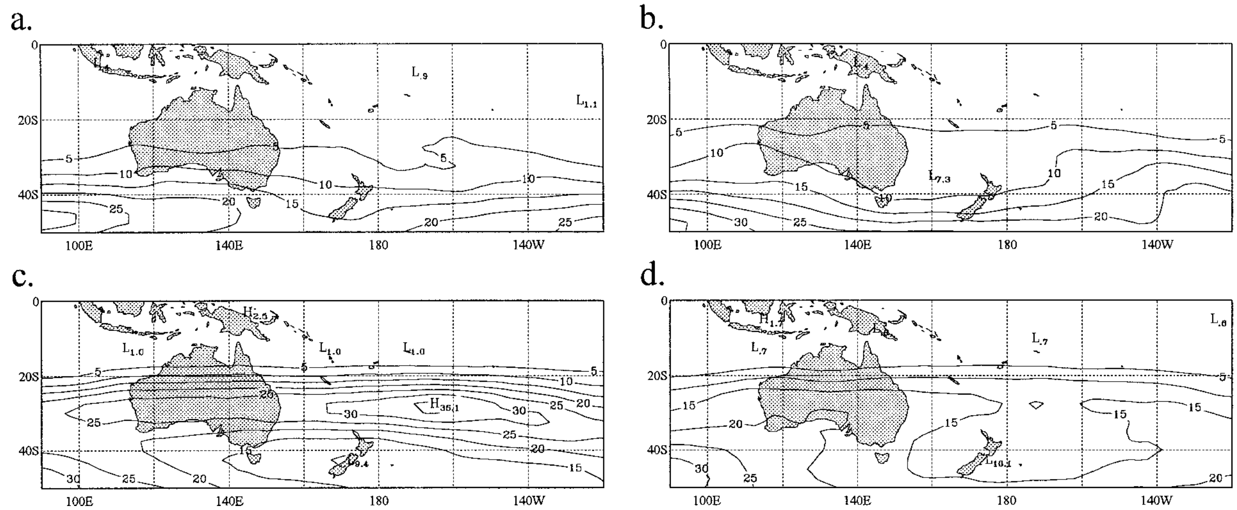

FIG. 2. Average vertically integrated mean kinetic energy (KM) in 10^5 J m^{-2} for (a) Jan, (b) Apr, (c) Jul, and (d) Oct.

k_m = vertical mean kinetic energy per unit mass

$$= \frac{1}{2}(\mathbf{V}_m \cdot \mathbf{V}_m),$$

k' = departure kinetic energy per unit mass

$$= \frac{1}{2}(\mathbf{V}' \cdot \mathbf{V}'), \quad \text{and}$$

k_s = vertical shear kinetic energy per unit mass

$$= \frac{1}{2}(\mathbf{V}' \cdot \mathbf{V}') + (\mathbf{V}_m \cdot \mathbf{V}').$$

The equations can be vertically integrated with respect to mass to yield:

$$\text{TKE} = \text{total kinetic energy} = \int_s \int_p k, \tag{6}$$

$$\text{KM} = \text{vertical mean kinetic energy} = \int_s \int_p k_m, \tag{7}$$

and

$$\text{KS} = \text{vertical shear kinetic energy}$$
$$= \int_s \int_p k_s = \int_s \int_p \frac{1}{2}(u'^2 + v'^2) \int_2 \int_p k', \tag{8}$$

where

$$\text{TKE} = \text{KM} + \text{KS}. \tag{9}$$

Wiin Nielson (1962) and subsequent authors have referred to KM and KS as the barotropic and baroclinic components, respectively; however, we have decided to use the terms vertical mean and vertical shear. When the vertical shear kinetic energy is integrated with respect to mass, the interaction term ($\mathbf{V}_m \cdot \mathbf{V}'$) disappears and KS becomes the vertical mass integral of the departure kinetic energy. Only when the shear kinetic energy is evaluated at a specific level does the interaction term apply. In the present study, monthly averages of TKE, KM, and KS are examined.

3. Results and discussion

Figures 2 and 3 show the vertically integrated KM and KS for the midseason months. The TKE patterns were similar to those of the 200-hPa zonal wind and, thus, are not shown. Both components show that significantly more energy is present in July than January. On the other hand, many contrasting features exist. First, KM generally seems to be greater than KS; however, it is only slightly greater, indicating that both types of kinetic energy are important. In January, KM does not have a well-defined axis of maximum values associated with the subtropical jet, whereas KS does, and the KS maximum located over the western South Pacific is larger than the KM values in the same region. The KS maximum is located in the entrance region of the western Pacific jet core (shown in Fig. 1a). This concurs with previous results by Feldstein and Held (1989) in their theoretical paper based on a two-layer model, and Ko and Vincent (1995) in their observational study where they found the entrance region of this jet core to be more baroclinic during the summer season.

In April, KS is still greater than KM in the entrance region of the western Pacific jet; however, in July and October, the values of KM are generally larger than those of KS along the entire jet stream. Nonetheless, during July, a maximum of KS is centered in the western Pacific at 30°S, 160°E, while a maximum of KM is centered in the central Pacific at 30°S, 160°W. The locations of these two maxima suggest that the results found by Ko and Vincent (1995) for the summertime western Pacific jet generally hold true for the wintertime

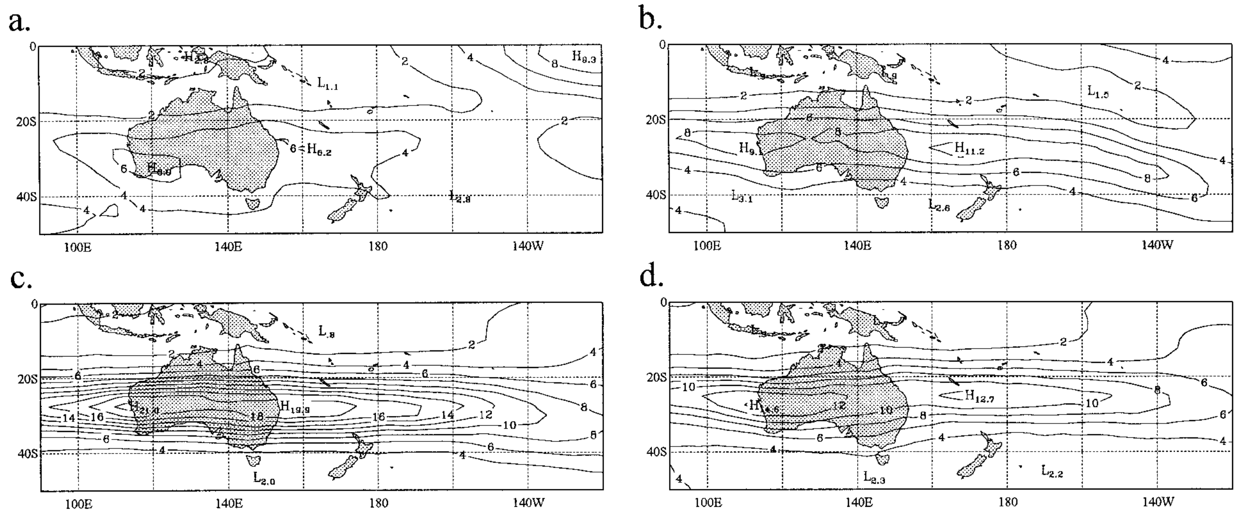

FIG. 3. Average vertically integrated shear kinetic energy (KS) in 10^5 J m^{-2} for (a) Jan, (b) Apr, (c) Jul, and (d) Oct.

jet core, as well. That is, along the axis of westerly maxima, the entrance region of the Pacific jet appears to have a greater percentage of shear kinetic energy than the exit region, whereas the exit region is dominated more by the mean kinetic energy component.

As discussed in section 2, kinetic energy at a specific level involves an internal shear term, as well as an interaction term that disappears in the vertically integrated results. It is of some interest, therefore, to explore the relative importance of these two terms at the jet stream level, that is, 200 hPa. Since the energy at this level cannot be mass weighted, the shear values are in units of 10 m^2 s^{-2}. Results were examined for each of the four midseason months during the 6-yr period. An example is shown for January 1989 in Fig. 4. It is seen that the internal shear term is slightly greater than the interaction term in the vicinity of the subtropical jet over the east coast of Australia. Also, the shear term dominates the equatorial westerly jet located in the northeast corner of the analysis region. In middle latitudes, however, the interaction term dominates. The patterns shown in Fig. 4 varied somewhat from one January to the next, depending on the latitude of maximum wind. For example, in January 1987, when the jet occurred over southeastern Australia (35°–40°S), the interaction term was twice as large as the internal shear term. It appeared, however, that this jet was an extension of the polar jet. In contrast, all of the July maps showed that both terms were important, with the interaction term being slightly greater, especially over the Pacific Ocean.

In order to examine the jet stream's kinetic energy variations in more detail, both spatially and temporally, the domain containing the average axis of maximum energy content (30°S) was partitioned into several regions across Australia and the South Pacific. Figure 5 shows these regions. Each region is indicated by a box that is 10° latitude × 20° longitude. Three-month running means of TKE, KM, and KS were averaged over each box. Time series of these quantities were examined for the 6-yr period of study; examples are shown for boxes 3 and 6 in Figs. 6 and 7. While KM is lightly shaded, KS is represented by dark shading. Also shown is the percentage of TKE that is contained in KS. Both boxes show a strong annual cycle, with maxima of TKE in July–August of each year and minima about 6 months later. It is worth noting that all regions, except the two most polar ones (boxes 8 and 10), showed a distinct annual cycle similar to those shown in Figs. 6 and 7. Both the seasonal swing and the TKE amounts were greater along 30°S (boxes 1–6) than for the two boxes (7 and 9) centered at 20°S, while the two boxes centered at 40°S showed the least seasonal variation, as noted above, and had TKE values slightly less than those along 30°S.

It is well known that an El Niño event occurred in 1986–87. During such an event, sea surface temperatures gradually increase across the central and eastern Pacific Ocean. As a result, anomalous convection shifts eastward into this region, causing strong upper-level divergent outflow. Some of this outflow travels southward and, under the action of the coriolis force, enhances the subtropical jet stream over the South Pacific (e.g., Ko and Vincent 1996). The El Niño event of 1986–87 is easily identified in Figs. 6 and 7, which show an eastward progression of the subtropical jet. The westernmost region (box 3) has maximum TKE during mid to late 1986, whereas box 6, which is centered 60° longitude farther east, has maxima lasting through to mid-1987.

Also evident in these two figures are two facts concerned with the percentage of TKE that is due to KS. First, it is seen that the larger percentage of KS is present in late summer when the TKE is at a minimum. This relationship was valid for all boxes, except 8 and 10,

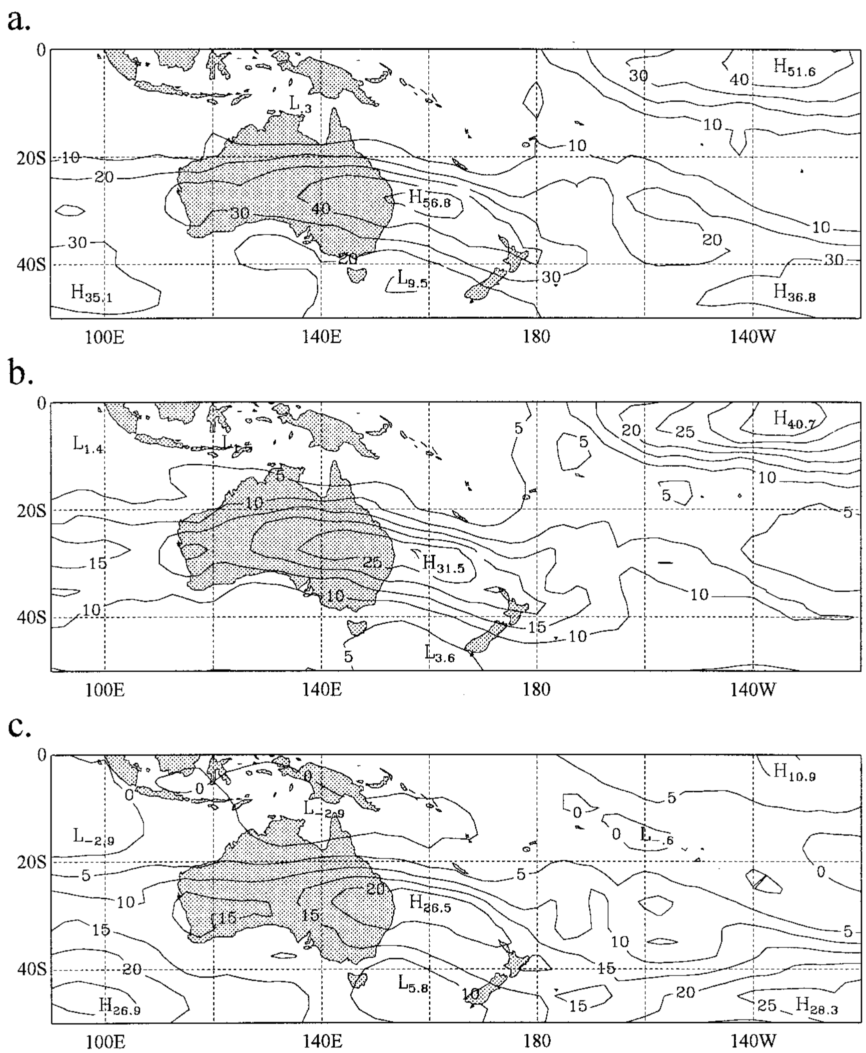

FIG. 4. Contribution of terms of shear kinetic energy at 200 hPa in $m^2\ s^{-2}$ for Jan 1989 where (a) is the total shear kinetic energy, (b) is the internal shear kinetic energy, and (c) is the interaction energy.

and ranged from 40% to 60% across the boxes centered on 30°S. The highest percentages occurred in boxes 7 and 9, while the lowest were in boxes 8 and 10. Second, the overall average for the 6-yr period is approximately 43% for box 3 and 33% for box 6. The longitudinal variation of the percentages along 30°S is depicted in Fig. 8. It is seen that the Australian–western Pacific area

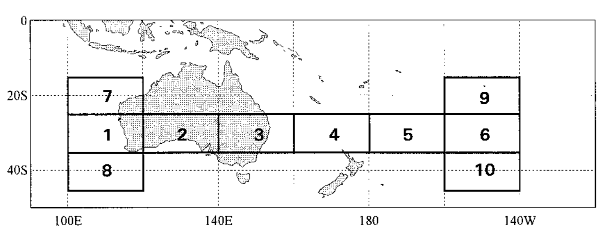

FIG. 5. Location of boxes 1–10.

has greater baroclinicity than the area over the central Pacific. This agrees with the findings of Ko and Vincent (1995, 1996). A third fact regarding the percentages, which is not shown in Figs. 6 and 7, is their latitudinal variation. The time series (not shown except for box 6) for boxes 7 and 9 (20°S), boxes 1 and 6 (30°S), and boxes 8 and 10 (40°S) indicated, somewhat surprisingly, that the Tropics in these regions had higher percentages of KS than the subtropics and much more KS than middle latitudes. This feature needs to be examined further.

One method to investigate the annual cycle of the kinetic energy content depicted in Figs. 6 and 7 is to compute an average annual cycle for the 6-yr period. For each of the 10 boxes shown in Fig. 5, the kinetic energy content for each month of the year was averaged over the 6-yr climatology (i.e., all six Januarys were averaged, etc.). This produced an average annual cycle

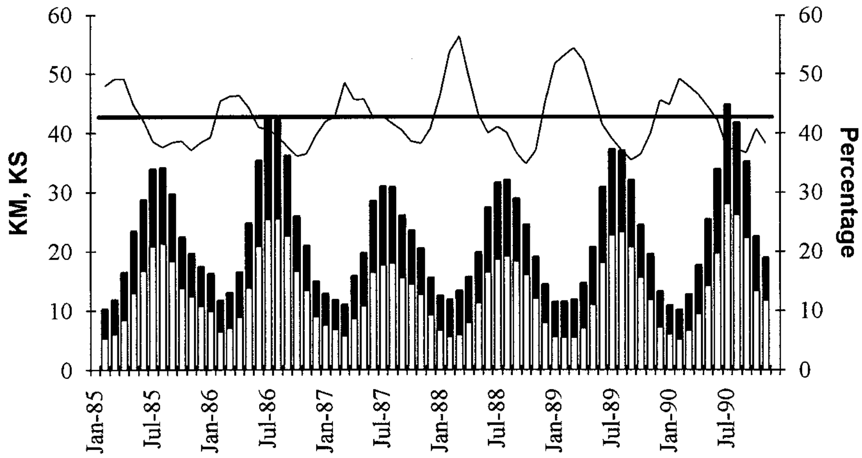

FIG. 6. Three-month running means of the vertically integrated KM and KS in 10^5 J m^{-2} for box 3. The percentage of the TKE represented by the shear kinetic energy is also shown, along with the average percentage during the 6-yr time period.

for each box in the form of bar graphs (not shown). These graphs included TKE, KM, and KS, as well as the percentage of the TKE represented by KS. The extremes of the annual cycles were compiled, together with other statistics, and are presented in Table 1. All 10 boxes depicted in Table 1 show an annual cycle in which the maximum TKE occurred in July and/or August, with the minimum occurring from January to March. Boxes 1–6, along the subtropical jet stream (30°S), contain the greatest kinetic energy, maximizing around 40×10^5 J m^{-2}. Boxes 7 and 9 (20°S) maximize at 20×10^5 J m^{-2}, with boxes 8 and 10 at $25–30 \times 10^5$ J m^{-2}. Boxes 1–6 also experience the greatest annual change, approximately 30×10^5 J m^{-2}, which is at least twice as much as the boxes at other latitudes.

Table 1 also shows that the boxes generally have their greatest KS percentage in March or April, with the minimum in September or October. These times correspond to when the jet stream is strengthening and weakening during its annual cycle. They also precede, by approximately 3 months, the maximum and minimum of the jet stream's kinetic energy. This suggests that vertical shear supports jet enhancement, while the vertically uniform flow favors decay. This was previously found by Wiin Nielson and Drake (1965), Feldstein and Held (1989), Ko and Vincent (1995), and Vincent et al. (1997). Along the jet stream axis, the Australian and western Pacific regions (boxes 2–4) are dominated by KS (>50%) during their maxima. Boxes 2–4 also have greater KS percentages year-round. This indicates that this region is favorable for jet enhancement, as well as maintenance, compared to the central Pacific (boxes 5 and 6) where KM dominates.

One way to investigate the interannual variability of a time series exhibiting a strong annual cycle is to remove the annual cycle from the time series. This was

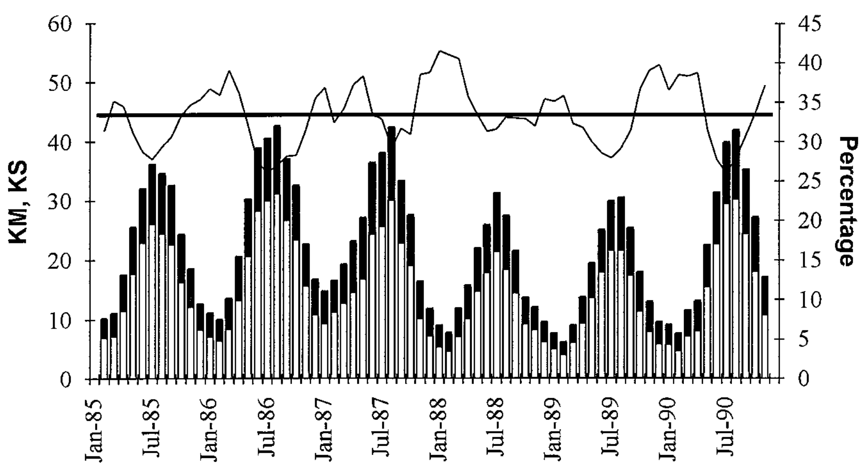

FIG. 7. Three-month running means of the vertically integrated KM and KS in 10^5 J m^{-2} for box 6. The percentage of the TKE represented by the shear kinetic energy is also shown, along with the average percentage during the 6-yr time period.

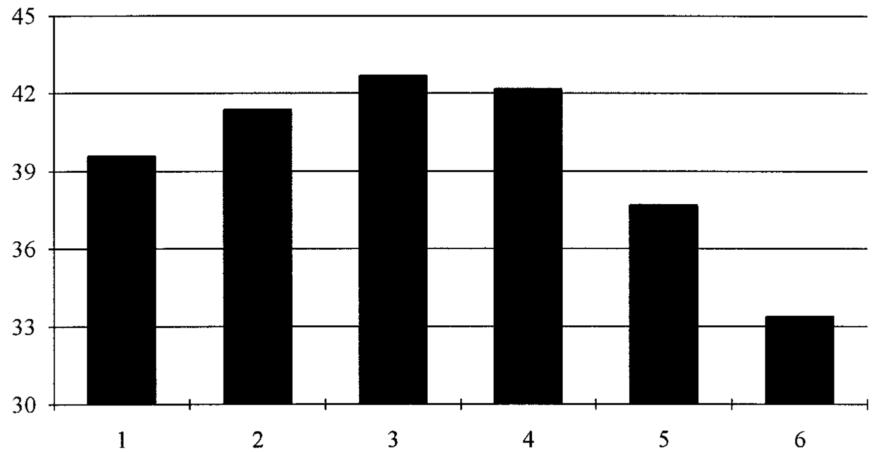

FIG. 8. The 6-yr average of the percentage of TKE represented by the KS for boxes 1–6.

done for TKE for all 10 boxes by subtracting the 6-yr average for a given month from each respective month. A sample of the resulting time series is shown for box 6 in Fig. 9. Positive values indicate a greater-than-normal value of TKE, and negative values indicate a less-than-normal value. The TKE for box 6 shows a positive anomaly in the central Pacific during the El Niño event of 1986–87 and experiences a negative anomaly of the same magnitude during the La Niña event of 1988–89. In contrast, boxes 1 and 2 (not shown) experienced a below-normal TKE during El Niño. The longitudinal variations in TKE from box 1 to box 6 showed a slow, but steady, eastward progression of the anomaly pattern during the ENSO cycle. This progression was in good agreement with similar anomalies of enhanced convection documented by Vincent and Schrage (1995) for the 1986–89 ENSO cycle. This further supports the theory that the enhancement of jet streams, and their respective kinetic energy contents, is frequently due to the supply of energy to the subtropics by the divergent outflow from the convective Tropics.

4. Summary and conclusions

In this study, the vertically averaged (mean) kinetic energy and shear kinetic energy were examined over the Australian–South Pacific region. In general, KM tended to slightly dominate over KS across the region; however, KS was dominant over KM in Australia and the western Pacific during the summer season. Even during the winter season when KM was dominant, the Australian–western Pacific area still contained a higher percentage of KS than the rest of the region to the east. The kinetic energy at the level of the jet stream (200 hPa), which contains two terms, the internal shear energy and the interaction energy, was independently analyzed. These two terms were found to be relatively equal in the region of the subtropical jet.

To quantify the longitudinal, as well as latitudinal, variations of kinetic energy, the subtropical jet domain was partitioned into 10 regions (boxes). Composite results of these boxes indicated that the subtropical jet experiences a strong annual cycle. The kinetic energy of the jet maximized in the winter and minimized in late summer. An out-of-phase relationship between the total kinetic energy and the percentage of the TKE represented by KS was found to exist, such that 1–3 months following the minimum of TKE (January–March), the greatest percent of KS was present (March–April). The percentage of KS was greater than 50% in the boxes over Australia and the western Pacific during these peak periods but was much less over the central Pacific. The

TABLE 1. Summary statistics of average annual cycles. Values of maximum and minimum total kinetic energy are in units of 10^5 J m^2.

Box	Central (°)	Max TKE		Min TKE		Max KS (%)		Min KS (%)	
1	30	Jul–Aug	39	Feb	10	Mar	44	Oct	36
2	30	Jul–Aug	41	Feb–Mar	11	Mar	52	Oct	35
3	30	Jul–Aug	41	Feb–Mar	11	Mar	53	Oct	34
4	30	Jul–Aug	41	Jan	11	Apr	52	Oct	33
5	30	Jul	43	Jan	9	Apr	45	Jul	31
6	30	Jul	40	Feb	9	Apr	39	Sep	30
7	20	Jul	19	Jan–Feb	4	Jan	62	Oct	46
9	20	Aug	19	Jan–Mar	5	Jan	53	Jul	36
8	40	Aug	28	Mar	20	Mar	19	Oct	15
10	40	Jul	24	Feb	15	Mar	24	Oct	17

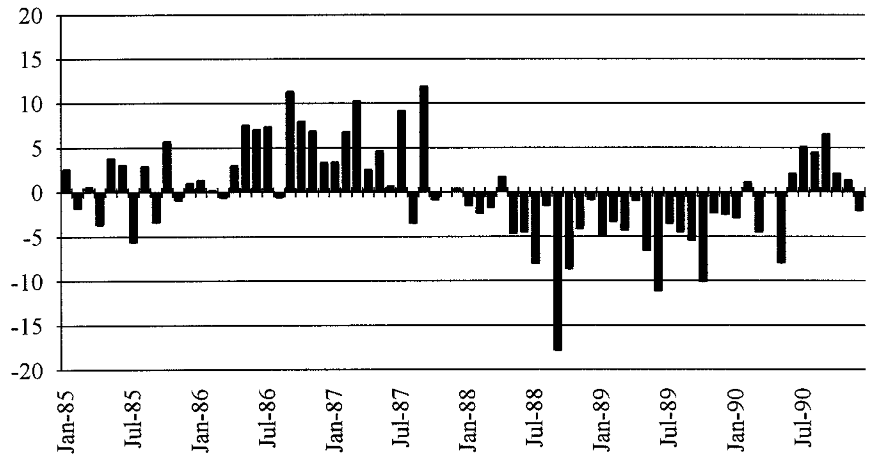

FIG. 9. Time series for TKE with the annual cycle removed in 10^5 J m^{-2} for box 6.

increase in KS in the jet's entrance region tended to coincide with the annual strengthening of the subtropical jet, suggesting that high values of baroclinicity in the jet's entrance region can lead to enhancement and maintenance of the subtropical jet.

The kinetic energy contents examined in this study experienced interannual variability, especially with regard to the El Niño–Southern Oscillation (ENSO) cycle of 1986–89. During the El Niño of 1986–87, TKE increased over the central Pacific, in conjunction with a decrease over Australia, a pattern that is in agreement with the jet moving eastward, as observed by Smith and Bromwich (1994) and Ko and Vincent (1996). During the La Niña of 1988–89, an opposite pattern of TKE occurred, as the jet retreated westward. Furthermore, the increase in TKE during El Niño was largely due to KM, while the increase during La Niña was due more to KS. This may be a reflection of the location of each maximum in relation to the jet's average entrance and exit regions, as well as the time of year that peak ENSO periods occurred.

The results of this study agree well with the results of Ko and Vincent (1995, 1996), although their studies were for summer seasons only. Furthermore, the results suggest good agreement with those of Wiin Nielson (1962), Chang and Lum (1985), and Vincent et al. (1997), in that high percentages of KS helped to enhance and maintain the jet. Hopefully, these results will provide some insight into the annual and interannual variability of the subtropical jet that may be useful in seasonal and year-to-year forecasting.

Acknowledgments. Most of this work was completed by the lead author as his undergraduate honors thesis for which he received first place in the AMS Macelwane Award competition. A debt of gratitude is due to a number of people and organizations. In particular, the authors thank Ms. Helen Henry, who typed the final manuscript; Messrs. Jon Schrage and Christopher Hennon, who provided healthy scientific discussions and technical advice; and Mr. Dan Vietor, who frequently assisted when computer programming problems arose. Part of Mr. Eastin's support came from a Barry M. Goldwater Scholarship, while Dr. Vincent's support was mainly due to National Science Foundation Grant ATM-9200534, issued to Purdue University. Much of the liaison and assistance in administering the grant came from the NOAA TOGA COARE Projects Office and from UCAR. The authors thank these organizations for their support.

REFERENCES

Chang, C.-P., and K. G. Lum, 1985: Tropical–midlatitude interactions over Asia and the western Pacific Ocean during the 1983/84 northern winter. *Mon. Wea. Rev.,* **113,** 1345–1358.

Feldstein, S. B., and I. M. Held, 1989: Barotropic decay of baroclinic waves in a two-layer beta-plane model. *J. Atmos. Sci.,* **46,** 3416–3430.

Huang, H.-J., and D. G. Vincent, 1983: Major changes in circulation features over the South Pacific during FGGE, 10–27 January 1979. *Mon. Wea. Rev.,* **111,** 1611–1618.

——, and ——, 1988: Active and inactive phases of the South Pacific convergence zone and changes in global circulation patterns: A case study. *Beitr. Phys. Atmos.,* **61,** 123–134.

Hurrell, J. W., and D. G. Vincent, 1990: Relationships between tropical heating and subtropical westerly maxima in the Southern Hemisphere during SOP-1, FGGE. *J. Climate,* **3,** 751–768.

——, and ——, 1991: On the maintenance of short-term subtropical wind maxima in the Southern Hemisphere during SOP-1, FGGE. *J. Climate,* **4,** 1009–1022.

Ko, K.-C., and D. G. Vincent, 1995: A composite study of the quasi-periodic subtropical wind maxima over the South Pacific during November 1984–April 1985. *J. Climate,* **8,** 579–588.

——, and ——, 1996: Behavior of one to two week summertime subtropical wind maxima over the South Pacific during an ENSO cycle. *J. Climate,* **9,** 5–16.

Nogues-Paegle, J., and Z. Zhen, 1987: The Australian subtropical jet during the second observing period of the Global Weather Experiment. *J. Atmos. Sci.,* **44,** 2277–2289.

——, and K. C. Mo, 1988: Transient response of the Southern Hemisphere subtropical jet to tropical forcing. *J. Atmos. Sci.,* **45,** 1493–1508.

Paegle, J., J. N. Paegle, and F. P. Lewis, 1983: Large-scale motion of the tropics in observations and theory. *Pure Appl. Geophys.,* **121,** 947–982.

Robertson, F. R., D. G. Vincent, and D. M. Kann, 1989: The role of diabatic heating in maintaining the upper-tropospheric baroclinic zone in the South Pacific. *Quart. J. Roy. Meteor. Soc.,* **115,** 1253–1271.

Smith, S. R., and D. H. Bromwich, 1994: Behavior of the tropospheric split jet stream over the South Pacific Ocean during the 1986–1989 ENSO cycle. Preprints, *Sixth Conf. on Climate Variations,* Nashville, TN, Amer. Meteor. Soc., 278–282.

Trenberth, K. E., 1986: An assessment of the impact of transient eddies on the zonal flow during a blocking episode using localized Eliassen–Palm flux diagnostics. *J. Atmos. Sci.,* **43,** 2070–2087.

——, 1987: The role of eddies in maintaining the westerlies in the Southern Hemisphere winter. *J. Atmos. Sci.,* **44,** 1498–1508.

——, 1992: Global analyses from ECMWF and atlas of 1000 to 10 mb circulation statistics. NCAR/TN-373+STR, National Center for Atmospheric Research, Boulder, CO, 191 pp. [Available from NCAR, Boulder, CO 80307.]

Vincent, D. G., 1985: Cyclone development in the South Pacific convergence zone during FGGE, 10–17 January 1979. *Quart. J. Roy. Meteor. Soc.,* **111,** 155–172.

——, and J. M. Schrage, 1994: Kinematic variables. Vol. 1, Climatology of the TOGA COARE and adjacent regions (1985–1990), 104 pp. [Available from Dept. of Earth and Atmospheric Sciences, Purdue University, West Lafayette, IN 47907.]

——, and ——, 1995: Thermodynamic and moisture variables. Vol. 2, Climatology of the TOGA COARE and adjacent regions (1985–1990), 123 pp. [Available from Dept. of Earth and Atmospheric Sciences, Purdue University, West Lafayette, IN 47907.]

——, K.-C. Ko, and J. M. Schrage, 1997: Subtropical jet streaks over the South Pacific. *Mon. Wea. Rev.,* **125,** 438–447.

Wiin Nielson, A., 1962: On transformation of kinetic energy between the vertical shear flow and the vertical mean flow in the atmosphere. *Mon. Wea. Rev.,* **90,** 313–323.

——, and M. Drake, 1965: On the energy exchange between the baroclinic and barotropic components of the atmospheric flow. *Mon. Wea. Rev.,* **93,** 79–92.